AAS 21-699

ANGULAR VELOCITY ESTIMATION USING RATE-INTEGRATING GYRO MEASUREMENTS

S.P. Arjun Ram*, Maruthi R. Akella†, and Renato Zanetti ‡

Rate Integrating Gyroscopes (RIGs) measure integrated angular rates or angular displacement, requiring an observer to provide full state feedback to the attitude controller. The problem of estimating the angular velocity of a rotating rigid body with known inertia and torque, using measurements from a rate integrating gyro is considered. A nonlinear observer is designed that uses only continuous-time RIG measurements and provides estimates of the angular velocity. Moreover, the observer is shown to be robust to bounded inaccuracies in the knowledge of inertia and external torque acting upon the system while the state estimation error converges exponentially to zero when the model is perfect. The observer is tested in simulation to demonstrate its effectiveness.

INTRODUCTION

Inertial navigation is a critical component of aerospace control systems for the calculation of position, velocity and orientation using measurements from Inertial Measurement Units (IMUs). These systems are usually comprised of accelerometers and gyroscopes and integrate forward in time the initial state of the vehicle by replacing dynamic models with IMU measurements. Inertial navigation systems have been used since the 1950s and were popularly part of the Apollo missions on the Saturn V rockets, the command module and the lunar module. In a strapdown inertial navigation system [1], the IMU is rigidly mounted on the vehicle. Strapdown gyroscopes have been used for many applications including spacecraft attitude estimation [2], underwater vehicle navigation [3], human navigation systems [4] and robotic navigation [5].

One approach to attitude determination is to integrate Euler's equation using models of the torques applied to the vehicle. Alternatively, inertial navigation bypasses the need for these models by measuring angular velocity directly (referred to as model replacement mode [6]). This methodology is preferred when IMU information is more accurate than the available models of rotational dynamics and torques. Moreover, model replacement is computationally much simpler for real-time onboard applications.

Rate Integrating Gyroscopes (RIGs) do not directly measure the angular rate but rather accumulate angular displacements by integrating the feedback required to null internal gyroscope motions. They provide measurements of the integrated rate and thus provide a direct measurement of neither

*Graduate Research Assistant, Department of Aerospace Engineering and Engineering Mechanics, The University of Texas at Austin. Email: arjun.ram@utexas.edu

†Ashley H. Priddy Centennial Professor, Department of Aerospace Engineering and Engineering Mechanics,The University of Texas at Austin. Email: makella@mail.utexas.edu, AIAA Associate Fellow, AAS Fellow

‡Assistant Professor, Department of Aerospace Engineering and Engineering Mechanics,The University of Texas at Austin. Email: renato@mail.utexas.edu, AIAA Associate Fellow, AAS Fellow

the attitude state nor the angular velocity. They are preferred in spacecraft applications compared to conventional rate gyroscopes for their low noise due to degenerate mode operation and exceptional scale factor stability [7]. Modern RIGs use micro-electromechanical system devices [8].

Attitude controllers for aerospace systems typically require state feedback, where the state consists of the attitude and angular rate. However, since rate integrating gyroscopes do not provide angular rate measurements, state feedback controllers would require an observer to reconstruct the full state using the IMU measurements. Kalman filters have been used in the literature to estimate this state [9,10]. For gyroscopes systems that measure angular velocity directly, nonlinear observers for attitude and gyro bias with exponential stability exist [11,12]. This work, on the other hand, focuses on designing an observer which uses continuous measurements from a RIG and provides estimates for the angular rate states that exponentially converge to their true values when the inertia of the body and the external torques are perfectly modeled. The angular velocity estimates provided by this observer can be used in controllers for stabilizing the system or tracking desired reference trajectories. To the best of our knowledge, no prior work exists in the literature on continuous time observers for RIGs systems.

RIGs are used for high precision applications because they provide the entire history of the angular velocity as its integrated value. The alternative of sampling the angular velocity at discrete times is typically less accurate as information on how the angular velocity varies in-between samples is lost. While we use continuous time RIG measurements here, discretizing the output of a continuous observer such as the one presented in this work will help use this observer with discrete time computer systems, while preserving the theoretical guarantees presented for the observer and the inherent advantages of using RIGs.

In this work, we consider a rigid body governed by Euler rotational dynamics and the angular rotational rate is assumed to satisfy a known upper bound. We present a nonlinear observer design which utilizes the measurements from the RIG and provides estimates of the angular rate states. The observer dynamics are linear in the measurement term and involve a user chosen parameter that controls the convergence rate. A Lyapunov-like analysis is used to prove that these state estimates exponentially converge to the true values of the angular velocity. Further, the observer is shown to be robust to inaccuracies in the inertia matrix and the external torque and the estimates converge to the true states within a residual set as long as the errors in inertia and torque are bounded. These results are demonstrated in numerical simulations.

The paper is organized as follows: the dynamics are introduced and the estimation problem is stated in the next section. The observer formulation and the Lyapunov-like analysis is presented for the convergence properties. The robustness of the observer to inertia and torque inaccuracies is then discussed in the following section. The simulation section follows, which performs numerical analysis of the observer system for the different scenarios before wrapping up with the conclusions in the final section. Throughout this paper, uppercase letters are used to denote matrices and bold faced variables denote vectors. For any symmetric matrix P, the notation $\lambda_{\min}(P)$ and $\lambda_{\max}(P)$ respectively denote the minimum and maximum eigenvalues.

PROBLEM DESCRIPTION

Dynamics

Consider Euler rotational dynamics for a system with inertia matrix $J = J^T > 0$ subject to bounded external torque $\boldsymbol{\tau}$ given by

$$J\dot{\boldsymbol{\omega}} = -\boldsymbol{\omega}^* J\boldsymbol{\omega} + \boldsymbol{\tau} \tag{1}$$

wherein $\boldsymbol{\omega}(t) \in \mathbb{R}^3$ has components in the body-fixed frame of reference. The skew-symmetric matrix $\boldsymbol{\omega}^*$ represents the vector cross product. We also assume:

- J is perfectly known
- $\boldsymbol{\tau}$ is perfectly determined
- $\boldsymbol{\omega} \in \mathbb{L}\infty$ is a bounded signal and we know $\omega_m \triangleq \sup_{t\geq 0} \|\boldsymbol{\omega}(t)\|$

The assumption that an upper bound ω_m is known is reasonable since any spacecraft is physically designed to only be able to rotate or tumble below a certain angular rate. The bound can be chosen beyond the design limits of the spacecraft.

Measurements

We have an RIG providing attitude measurements $\boldsymbol{\sigma}(t) \in \mathbb{R}^3$ which are the integrated values of the angular rate $\boldsymbol{\omega}$:

$$\dot{\boldsymbol{\sigma}} = \boldsymbol{\omega} \tag{2}$$

where $\boldsymbol{\sigma}(t)$ is assumed to be measured perfectly.

Objective

Using perfect measurements of $\boldsymbol{\sigma}(t)$, the goal is to generate an estimate $\hat{\boldsymbol{\omega}}(t)$ of the true angular rate $\boldsymbol{\omega}(t)$ such that

$$\lim_{t\to\infty} \|\hat{\boldsymbol{\omega}}(t) - \boldsymbol{\omega}(t)\| = 0 \tag{3}$$

keeping all signals bounded.

OBSERVER DESIGN

The following observer design is proposed for estimating the angular rate:

$$\dot{\hat{\boldsymbol{\sigma}}} = \hat{\boldsymbol{\omega}} - k(\hat{\boldsymbol{\sigma}} - \boldsymbol{\sigma}) \quad \text{for some } k > 0 \tag{4}$$

$$J\dot{\hat{\boldsymbol{\omega}}} = -\hat{\boldsymbol{\omega}}^* J\hat{\boldsymbol{\omega}} + \boldsymbol{\tau} - k^2 J(\hat{\boldsymbol{\sigma}} - \boldsymbol{\sigma}) \tag{5}$$

We define the estimation errors

$$\boldsymbol{\sigma}_e = \hat{\boldsymbol{\sigma}} - \boldsymbol{\sigma} \tag{6}$$

$$\boldsymbol{\omega}_e = \hat{\boldsymbol{\omega}} - \boldsymbol{\omega} \tag{7}$$

Using these definitions in (4)-(5) gives

$$\dot{\boldsymbol{\sigma}}_e = \boldsymbol{\omega}_e - k\boldsymbol{\sigma}_e \tag{8}$$

$$J\dot{\boldsymbol{\omega}}_e = (\hat{\boldsymbol{\omega}}^* J\hat{\boldsymbol{\omega}} - \boldsymbol{\omega}^* J\boldsymbol{\omega}) - k^2 J\boldsymbol{\sigma}_e \tag{9}$$

Expanding the terms within the parenthesis on the right-hand side of (9) gives

$$\hat{\boldsymbol{\omega}}^* J\hat{\boldsymbol{\omega}} - \boldsymbol{\omega}^* J\boldsymbol{\omega} = \boldsymbol{\omega}_e^* J\boldsymbol{\omega} + \boldsymbol{\omega}^* J\boldsymbol{\omega}_e + \boldsymbol{\omega}_e^* J\boldsymbol{\omega}_e \tag{10}$$

If we define $\boldsymbol{\Psi} \triangleq [\boldsymbol{\omega}^* J\boldsymbol{\omega}_e + \boldsymbol{\omega}_e^* J\boldsymbol{\omega} + \boldsymbol{\omega}_e^* J\boldsymbol{\omega}_e]$, (9) can be rewritten as

$$\dot{\boldsymbol{\omega}}_e = -k^2\boldsymbol{\sigma}_e + J^{-1}\boldsymbol{\Psi} \tag{11}$$

If we define the error states to be $\boldsymbol{\sigma}_e$ and $\boldsymbol{\omega}_e/k$, using (4) and (11), we have the dynamics for the error states as:

$$\begin{bmatrix} \dot{\boldsymbol{\sigma}}_e \\ \frac{\dot{\boldsymbol{\omega}}_e}{k} \end{bmatrix} = k \begin{bmatrix} -\mathbb{I}_{3\times3} & \mathbb{I}_{3\times3} \\ -\mathbb{I}_{3\times3} & \mathbb{O}_{3\times3} \end{bmatrix} \begin{bmatrix} \boldsymbol{\sigma}_e \\ \frac{\boldsymbol{\omega}_e}{k} \end{bmatrix} + \begin{bmatrix} \mathbb{O}_{3\times1} \\ \frac{J^{-1}}{k}\boldsymbol{\Psi} \end{bmatrix} \tag{12}$$

Renaming the states as

$$\begin{matrix} \boldsymbol{z}_1 = \boldsymbol{\sigma}_e \\ \boldsymbol{z}_2 = \frac{\boldsymbol{\omega}_e}{k} \end{matrix} \quad \Leftrightarrow \quad \boldsymbol{z} \triangleq \begin{bmatrix} \boldsymbol{z}_1 \\ \boldsymbol{z}_2 \end{bmatrix} \in \mathbb{R}^6$$

allows us to express (12) as

$$\dot{\boldsymbol{z}} = k \begin{bmatrix} -\mathbb{I}_{3\times3} & \mathbb{I}_{3\times3} \\ -\mathbb{I}_{3\times3} & \mathbb{O}_{3\times3} \end{bmatrix} \boldsymbol{z} + \begin{bmatrix} \mathbb{O}_{3\times1} \\ \frac{J^{-1}}{k}\boldsymbol{\Psi} \end{bmatrix} \tag{13}$$

Since the inertia matrix is known, we can use its maximum and minimum eigenvalues to express

$$J_M = \lambda_{\max}(J) = \|J\| \tag{14}$$

$$J_m = \lambda_{\min}(J) = \frac{1}{\|J^{-1}\|} \tag{15}$$

Define

$$\alpha \triangleq (J_M/J_m) \tag{16}$$

Revisiting the $\boldsymbol{\Psi}$ term introduced after Eq. 10, we have

$$\boldsymbol{\Psi} = \boldsymbol{\omega}^* J\boldsymbol{\omega}_e + \boldsymbol{\omega}_e^* J\boldsymbol{\omega} + \boldsymbol{\omega}_e^* J\boldsymbol{\omega}_e \tag{17}$$

$$\frac{J^{-1}}{k}\boldsymbol{\Psi} = \frac{J^{-1}}{k}(\boldsymbol{\omega}^* J\boldsymbol{\omega}_e + \boldsymbol{\omega}_e^* J\boldsymbol{\omega}) + \frac{J^{-1}}{k}\boldsymbol{\omega}_e^* J\boldsymbol{\omega}_e \tag{18}$$

Consider the norm of the first term

$$\|\frac{J^{-1}}{k}(\boldsymbol{\omega}^* J\boldsymbol{\omega}_e + \boldsymbol{\omega}_e^* J\boldsymbol{\omega})\| \leq \frac{2J_M}{kJ_m}\omega_m\|\boldsymbol{\omega}_e\| = \frac{2\alpha\omega_m\|\boldsymbol{\omega}_e\|}{k} = 2\alpha\omega_m\|z_2\| \tag{19}$$

Next,

$$\|\frac{J^{-1}}{k}\boldsymbol{\omega}_e^* J\boldsymbol{\omega}_e\| \leq \frac{1}{kJ_m}\sqrt{J_M(J_M - J_m)}\|\boldsymbol{\omega}_e\|^2 = k\sqrt{\alpha(\alpha-1)}\|\boldsymbol{z}_2\|^2 \tag{20}$$

Thus, making use of the bounds calculated in Eq. 19 and 20 and substituting them in Eq. 18 results in

$$\|\frac{J^{-1}\Psi}{k}\| \leq 2\alpha\omega_m\|z_2\| + k\sqrt{\alpha(\alpha-1)}\|z_2\|^2 \tag{21}$$

Convergence Analysis

For stability and convergence analysis, consider a Lyapunov-like candidate function

$$\begin{aligned} V &= \frac{1}{k}\left[\boldsymbol{z}_1^T\boldsymbol{z}_1 + \frac{3}{2}\boldsymbol{z}_2^T\boldsymbol{z}_2 - \boldsymbol{z}_1^T\boldsymbol{z}_2\right] \\ &= \begin{bmatrix}\boldsymbol{z}_1 & \boldsymbol{z}_2\end{bmatrix} \underbrace{\frac{1}{k}\begin{bmatrix}\mathbb{I}_{3\times3} & -\frac{1}{2}\mathbb{I}_{3\times3} \\ -\frac{1}{2}\mathbb{I}_{3\times3} & \frac{3}{2}\mathbb{I}_{3\times3}\end{bmatrix}}_{P\in\mathbb{R}^{6\times6}} \begin{bmatrix}\boldsymbol{z}_1 \\ \boldsymbol{z}_2\end{bmatrix} \\ &= \begin{bmatrix}\boldsymbol{z}_1 & \boldsymbol{z}_2\end{bmatrix} \left(\underbrace{\frac{1}{k}\begin{bmatrix}1 & -\frac{1}{2} \\ -\frac{1}{2} & \frac{3}{2}\end{bmatrix}}_{R\in\mathbb{R}^{2\times2}} \otimes \mathbb{I}_{3\times3}\right) \begin{bmatrix}\boldsymbol{z}_1 \\ \boldsymbol{z}_2\end{bmatrix} \end{aligned} \tag{22}$$

where $\otimes$ denote the Kronecker product.

We know the maximum and minimum eigenvalues of P and R are equal: $\lambda_{\min}(P) = \lambda_{\min}(R)$ and $\|P\| = \lambda_{\max}(P) = \lambda_{\max}(R)$ which gives us

$$\lambda_{\min}(P) = \frac{5-\sqrt{5}}{4k} = c_1 \tag{23}$$

and

$$\lambda_{\max}(P) = \frac{5+\sqrt{5}}{4k} = c_2 \tag{24}$$

Thus, V defined in Eq. (22) satisfies

$$c_1\|\boldsymbol{z}\|^2 \leq V = \boldsymbol{z}^T P \boldsymbol{z} \leq c_2\|\boldsymbol{z}\|^2 \tag{25}$$

Next, taking the time derivative of V in Eq. (22), followed by substituting Eq. 13 and Eq. 18 results in

$$\begin{aligned} \dot{V} &= \frac{2}{k}\boldsymbol{z}_1^T\dot{\boldsymbol{z}}_1 + \frac{3}{k}\boldsymbol{z}_2^T\dot{\boldsymbol{z}}_2 - \frac{1}{k}\boldsymbol{z}_1^T\dot{\boldsymbol{z}}_2 - \frac{1}{k}\boldsymbol{z}_2^T\dot{\boldsymbol{z}}_1 \\ &= -\boldsymbol{z}_1^T\boldsymbol{z}_1 - \boldsymbol{z}_2^T\boldsymbol{z}_2 + \frac{3}{k}\boldsymbol{z}_2^T\frac{J^{-1}\boldsymbol{\Psi}}{k} - \frac{1}{k}\boldsymbol{z}_1^T\frac{J^{-1}\boldsymbol{\Psi}}{k} \\ &\leq -\|\boldsymbol{z}\|^2 + \frac{3}{k}\|\boldsymbol{z}_2\|\|\frac{J^{-1}\boldsymbol{\Psi}}{k}\| + \frac{1}{k}\|\boldsymbol{z}_1\|\|\frac{J^{-1}\boldsymbol{\Psi}}{k}\| \\ &\leq -\|\boldsymbol{z}\|^2 + \frac{4}{k}\|\boldsymbol{z}\|\|\frac{J^{-1}\boldsymbol{\Psi}}{k}\| \end{aligned} \tag{26}$$

Next, using (19) and (20), we have

$$\begin{aligned} \dot{V} &\leq -\|\boldsymbol{z}\|^2 + \frac{4}{k}\|\boldsymbol{z}\|\left[2\alpha\omega_m\|\boldsymbol{z}\| + k\sqrt{\alpha(\alpha-1)}\|\boldsymbol{z}\|^2\right] \\ &= -\left(1 - \frac{8\alpha\omega_m}{k}\right)\|\boldsymbol{z}\|^2 + 4\sqrt{\alpha(\alpha-1)}\|\boldsymbol{z}\|^3 \end{aligned} \tag{27}$$

To ensure the coefficient of the $\|\boldsymbol{z}\|^2$ term is negative, we select k such that $1 - (8\alpha\omega_m)/k > 0$, i.e.,

$$k > 8\alpha\omega_m \tag{28}$$

In other words, $k^* \triangleq 8\alpha\omega_m$ and $k > k^*$. Thus, we have

$$\begin{aligned}
\dot{V} &\leq -\left(1 - \frac{8\alpha\omega_m}{k}\right)\|\boldsymbol{z}\|^2 + 4\beta\|\boldsymbol{z}\|^3 \\
\dot{V} &\leq -\|\boldsymbol{z}\|^2\left[\left(1 - \frac{8\alpha\omega_m}{k}\right) - 4\beta\|\boldsymbol{z}\|\right] \\
&\triangleq -W(\boldsymbol{z})
\end{aligned} \tag{29}$$

where we introduce the notation $\beta = \sqrt{\alpha(\alpha - 1)}$

Define a scalar function $\rho(k)$:

$$\rho(k) \triangleq \frac{1}{4\beta}\left(1 - \frac{8\alpha\omega_m}{k}\right)\sqrt{\frac{c_1}{c_2}} \tag{30}$$

which after substituting the values of c_1 and c_2 respectively from (23) and (24) becomes

$$\rho(k) = \frac{1}{4\beta}\left(1 - \frac{8\alpha\omega_m}{k}\right)\sqrt{\frac{5 - \sqrt{5}}{5 + \sqrt{5}}} \tag{31}$$

Suppose we restrict initial conditions $\boldsymbol{z}(t_0)$ at time $t_0 = 0$, such that $\|\boldsymbol{z}(t_0)\| \leq \rho(k)$, then using Eq. 29,

$$\begin{aligned}
W(\boldsymbol{z}(0)) &= \|\boldsymbol{z}(0)\|^2\left[\left(1 - \frac{8\alpha\omega_m}{k}\right) - 4\beta\|\boldsymbol{z}(0)\|\right] \\
&= 4\beta\|\boldsymbol{z}(0)\|^2\left[\frac{1}{4\beta}\left(1 - \frac{8\alpha\omega_m}{k}\right) - \|\boldsymbol{z}\|\right] \\
&\geq 4\beta\|\boldsymbol{z}(0)\|^2\left[\rho(k)\sqrt{\frac{c_2}{c_1}} - \rho(k)\right] \\
&\geq 0
\end{aligned} \tag{32}$$

since $c_2 > c_1$.

By definition of $W(\boldsymbol{z})$ in Eq. 29, we know that $\dot{V}(t) \leq 0$ whenever $W(\boldsymbol{z}(t)) \geq 0$. Thus, having $\|\boldsymbol{z}(0)\| \leq \rho(k)$ ensures $\dot{V}(t) \leq 0$ for all $t \geq 0$, that is, $V(t)$ is non-increasing with time. Substituting this in (25) leads to

$$c_1\|\boldsymbol{z}(t)\|^2 \leq V(t) \leq V(0) \leq c_2\|\boldsymbol{z}(0)\|^2 \tag{33}$$

Thus,

$$\|\boldsymbol{z}(t)\| \leq \sqrt{\frac{c_2}{c_1}}\|\boldsymbol{z}(0)\| \tag{34}$$

Also, using the definition of $W(\boldsymbol{z})$ from (29),

$$\begin{aligned} W(\boldsymbol{z}(t)) &= \|\boldsymbol{z}(t)\|^2 \left[\left(1 - \frac{8\alpha\omega_m}{k} \right) - 4\beta \|\boldsymbol{z}(t)\| \right] \\ &\geq \|\boldsymbol{z}(t)\|^2 \left[\left(1 - \frac{8\alpha\omega_m}{k} \right) - 4\beta \sqrt{\frac{c_2}{c_1}} \|\boldsymbol{z}(0)\| \right] \end{aligned}$$

Defining c_3 to be the terms inside the square brackets,

$$-W(\boldsymbol{z}(t)) \leq -c_3 \|\boldsymbol{z}(t)\|^2 \tag{35}$$

Thus we have $\dot{V}(t) \leq -W(\boldsymbol{z}(t)) \leq -c_3 \|\boldsymbol{z}(t)\|^2$ or,

$$\begin{aligned} \dot{V}(t) &\leq -\frac{c_3}{c_2} V(t) \\ V(t) &\leq \exp\left(\frac{-c_3 t}{c_2} \right) V(0) \end{aligned} \tag{36}$$

Using this result alongside the inequality from (25) results in

$$\|\boldsymbol{z}(t)\| \leq \sqrt{\frac{c_2}{c_1}} \exp\left(\frac{-c_3 t}{2c_2} \right) \|\boldsymbol{z}(0)\| \tag{37}$$

which proves exponential stability but is a local result for $\|\boldsymbol{z}(0)\| \leq \rho(k)$

Discussion

For choosing the value of k, from Eq. 28 we have a lower bound $k^* = 8\alpha\omega_m$. From (23) and (24) we know, as $k \to \infty$, both $c_1 \to 0$ and $c_2 \to 0$.

However, the ratio

$$\sqrt{\frac{c_1}{c_2}} = \sqrt{\frac{5 - \sqrt{5}}{5 + \sqrt{5}}} \tag{38}$$

is independent of k.

The upper bound on the initial value of $\|\boldsymbol{z}(0)\|$ is

$$\rho(k) = \frac{1}{4\beta} \left[1 - \frac{8\alpha\omega_m}{k} \right] \sqrt{\frac{c_1}{c_2}} \tag{39}$$

which in the limit becomes

$$\lim_{k \to \infty} \rho(k) = \rho^* = \frac{1}{4\beta} \sqrt{\frac{c_1}{c_2}} = \frac{1}{4\beta} \sqrt{\frac{5 - \sqrt{5}}{5 + \sqrt{5}}} \tag{40}$$

Thus, the bound on the initial condition is bounded for any chosen value of k.

Note that local stability implies specifically, our initial condition $\boldsymbol{z}(0) \in \mathbb{M}$ where

$$\mathbb{M} = \left\{ \boldsymbol{z} \in \mathbb{R}^6 \quad | \quad \|\boldsymbol{\sigma}_e(0)\|^2 + \frac{\|\boldsymbol{\omega}_e(0)\|^2}{k^2} \leq \rho^2(k) \right\} \tag{41}$$

which is the region of attraction. $\boldsymbol{\sigma}_e(0)$ is usually not a restriction because, we can always select $\hat{\boldsymbol{\sigma}}(0) = \boldsymbol{\sigma}(0) \Leftrightarrow \boldsymbol{\sigma}_e(0) = 0$

On the other hand, $\boldsymbol{\omega}_e(0)$ can be arbitrarily large. However, we can always choose large enough k such that irrespective of $\boldsymbol{\omega}_e(t)$,$\boldsymbol{z}(0) \in \mathbb{M}$. In this context, it is crucial that

$$\lim_{k\to\infty} \rho(k) = \rho^* = \text{finite constant}$$

Hence, the result is semi-global.

Convergence Rate

In (37), $(-c_3/2c_2)$ is the rate of convergence. Note that

$$c_3 = \left(1 - \frac{8\alpha\omega_m}{k}\right) - 4\beta\sqrt{\frac{c_2}{c_1}}\|\boldsymbol{z}(0)\| \tag{42}$$

Thus, as $k \to \infty$, $c_3 \to c_3^*$ where

$$c_3^* = 1 - 4\beta\sqrt{\frac{5+\sqrt{5}}{5-\sqrt{5}}}\|\boldsymbol{z}(0)\| \tag{43}$$

which is independent of k. Also recall that $c_2 \to 0$ as $k \to \infty$. Thus, the rate of convergence $(c_3/2c_2) \to \infty$ as $k \to \infty$. Thus selecting large k implies faster convergence.

ROBUSTNESS ANALYSIS

We consider two different scenarios:

- The external torque $\boldsymbol{\tau}$ is unavailable but is bounded and an upper bound is known $\boldsymbol{\tau} \in \mathbb{L}_\infty$, i.e., there exists some finite $\tau_m = \sup_{t\geq 0} \|\boldsymbol{\tau}(t)\|$. Can the observer be ensured to converge to a residual set?
- The inertia matrix J is inaccurately modelled as $\bar{J} = \bar{J}^T > 0$ (nominal inertia) and thus, there is an inertia error $(J - \bar{J})$? Can the observer errors be bounded in this setting?

We provide positive answers to both these cases in the sequel.

Unknown Torque

We assume some bounded unknown external torque $\boldsymbol{\tau}$ acting upon the spacecraft. The observer is modified to:

$$\dot{\hat{\boldsymbol{\sigma}}} = \hat{\boldsymbol{\omega}} - k(\hat{\boldsymbol{\sigma}} - \boldsymbol{\sigma}) \tag{44}$$

$$J\dot{\hat{\boldsymbol{\omega}}} = -\hat{\boldsymbol{\omega}}^* J\hat{\boldsymbol{\omega}} - k^2 J(\hat{\boldsymbol{\sigma}} - \boldsymbol{\sigma}) \tag{45}$$

This leads to

$$\dot{\boldsymbol{\sigma}}_e = -k\boldsymbol{\sigma}_e + k\left(\frac{\boldsymbol{\omega}_e}{k}\right) \tag{46}$$

$$\frac{\dot{\boldsymbol{\omega}}_e}{k} = -k\boldsymbol{\sigma}_e + \frac{J^{-1}}{k}\boldsymbol{\Psi} - \frac{J^{-1}}{k}\boldsymbol{\tau} \tag{47}$$

$$\Leftrightarrow \dot{\boldsymbol{z}} = k\begin{bmatrix} -\mathbb{I} & \mathbb{I} \\ -\mathbb{I} & 0 \end{bmatrix}\boldsymbol{z} + \begin{bmatrix} 0 \\ \frac{J^{-1}}{k}\boldsymbol{\Psi} \end{bmatrix} + \begin{bmatrix} 0 \\ -\frac{J^{-1}}{k}\boldsymbol{\tau} \end{bmatrix} \tag{48}$$

where the last term is defined as the disturbance

$$\boldsymbol{d} \triangleq \begin{bmatrix} 0 \\ -\frac{J^{-1}}{k}\boldsymbol{\tau} \end{bmatrix} \tag{49}$$

For the case with known torque ($\boldsymbol{d} = 0$), we already have from Eq. 35, a Lyapunov function such that

$$c_1\|\boldsymbol{z}\|^2 \leq V(\boldsymbol{z}) \leq c_2\|\boldsymbol{z}\|^2 \tag{50}$$

$$\dot{V} \triangleq \left(\frac{\partial V}{\partial z}\right)^T \dot{\boldsymbol{z}} \leq -c_3\|\boldsymbol{z}\|^2 \tag{51}$$

Also recall

$$V(\boldsymbol{z}) = \frac{1}{k}\left(\boldsymbol{z}_1^T\boldsymbol{z}_1 + \frac{3}{2}\boldsymbol{z}_2^T\boldsymbol{z}_2 - \boldsymbol{z}_1^T\boldsymbol{z}_2\right) = \boldsymbol{z}^T P\boldsymbol{z} \tag{52}$$

Thus, $\frac{\partial V}{\partial z} = 2P\boldsymbol{z}$

$$\Leftrightarrow \|\frac{\partial V}{\partial z}\| \leq 2\lambda_{\max}(P)\|\boldsymbol{z}\| = 2c_2\|\boldsymbol{z}\| \tag{53}$$

since $\|P\| = \lambda_{\max}(P) = c_2 = (5+\sqrt{5})/4k$.

If we define $c_4 = 2c_2$, the above equation can be written as $\|\frac{\partial V}{\partial z}\| \leq c_4\|\boldsymbol{z}\|$. Next recall,

$$\boldsymbol{d} = \begin{bmatrix} 0 \\ -\frac{J^{-1}}{k}\boldsymbol{\tau} \end{bmatrix} \Leftrightarrow \|\boldsymbol{d}\| \leq \frac{\tau_m}{kJ_m} \tag{54}$$

Suppose for some $\theta \in (0,1)$,

$$\frac{\tau_m}{kJ_m} < \frac{c_3}{c_4}\sqrt{\frac{c_1}{c_2}}\theta\rho(k) \tag{55}$$

this implies that there exists k sufficiently large such that

$$\tau_m < \frac{c_3}{c_4}\sqrt{\frac{c_1}{c_2}}\theta k J_m\rho(k) \tag{56}$$

Then using Lemma 9.2 from Khalil [13], for all $\|\boldsymbol{z}(0)\| < \sqrt{c_1/c_2}\rho(k)$, we have

$$\|\boldsymbol{z}(t)\| \leq \sqrt{\frac{c_2}{c_1}}\exp\left(-\gamma(t)\right)\|\boldsymbol{z}(0)\| \quad \forall\, 0 \leq t \leq T \tag{57}$$

and

$$\|\boldsymbol{z}(t)\| \leq b \text{ for } t \geq T \tag{58}$$

which is a residual set and a uniform ultimate bound for some finite $T > 0$, where

$$\gamma = \frac{(1-\theta)c_3}{2c_2} \tag{59}$$

and

$$b = \frac{c_4}{c_3}\sqrt{\frac{c_2}{c_1}}\frac{\tau_m}{J_m k\theta} \tag{60}$$

note that $b \to 0$ as $k \to \infty$.

Inaccurate Inertia Model

If the inertia matrix J is poorly modeled, a nominal inertia $\bar{\boldsymbol{J}}$ is adopted with maximum and minimum eigenvalues $\bar{J}_M$ and $\bar{J}_m$ respectively. We modify the observer to be:

$$\dot{\hat{\boldsymbol{\sigma}}} = \hat{\boldsymbol{\omega}} - k(\hat{\boldsymbol{\sigma}} - \boldsymbol{\sigma}) \tag{61}$$

$$\dot{\hat{\boldsymbol{\omega}}} = -k^2(\hat{\boldsymbol{\sigma}} - \boldsymbol{\sigma}) - \bar{J}^{-1}\hat{\boldsymbol{\omega}}^* \bar{J}\hat{\boldsymbol{\omega}} + \bar{J}^{-1}\boldsymbol{\tau} \tag{62}$$

such that the disturbance term in Eq. 49 can be modified as follows

$$\bar{\boldsymbol{d}} = \begin{bmatrix} 0 \\ -\frac{1}{k}(\bar{J}^{-1}\boldsymbol{\omega}^* \bar{J}\boldsymbol{\omega} - J^{-1}\boldsymbol{\omega}^* J\boldsymbol{\omega}) + (\bar{J}^{-1} - J^{-1})\tau) \end{bmatrix} \tag{63}$$

The nominal system, i.e., with $\bar{\boldsymbol{d}} = 0$, provides us with the same behavior as the unknown torque case above, hence (57) and (58) hold with the convergence rate in (59). However, the modified ratio of eigenvalues of the inertia matrix, α is replaced by $\bar{\alpha} = \bar{J}_M/\bar{J}_m$ and the residual set to which the norm of the states converges to is now:

$$b = \frac{c_4}{c_3}\sqrt{\frac{c_2}{c_1}}\frac{1}{J_m \bar{J}_m k\theta}\left[\tau_m(\bar{J}_m + J_m) + \omega_m^2(J_M \bar{J}_m + \bar{J}_M J_m)\right] \tag{64}$$

This proves that the proposed observer is robust to inaccuracies in the inertia matrix and unknown external torques, with the angular velocity estimates always converging to a local residual region surrounding the true value of the state.

SIMULATIONS

We perform numerical simulations for a body starting from $\boldsymbol{\omega(0)} = [0.1, 0.05, 0]^T$ with inertia matrix

$$J = \begin{bmatrix} 20 & 1.2 & 0.9 \\ 1.2 & 17 & 1.4 \\ 0.9 & 1.4 & 15 \end{bmatrix} \tag{65}$$

The external torque is chosen as

$$\boldsymbol{\tau} = \begin{bmatrix} 0.1\sin(t) \\ 0.2\cos(2t) \\ 0.3\cos(3t) \end{bmatrix} \tag{66}$$

For the case when the inertia and torque are known accurately, the velocity and error in velocity are shown in Fig. 1, where the estimate can be clearly seen to be converging to the real value of the angular velocity and the error goes to zero.

For demonstrating the robustness properties of the observer, the system with the same inertia as Eq.65 with the observer using an inertia estimate of

$$\bar{J} = \begin{bmatrix} 21 & 2.2 & 1.9 \\ 2.2 & 18 & 2.4 \\ 1.9 & 2.4 & 16 \end{bmatrix} \tag{67}$$

which represents approximately 5% error in the inertia parameter model. The torque input from Eq. 66 was applied to the system but is unknown to the observer. The angular velocity and norm of the error states are shown in Fig. 2, where once again, the estimate converges to the true state, demonstrating the robustness of the observer to inertia and torque inaccuracies.

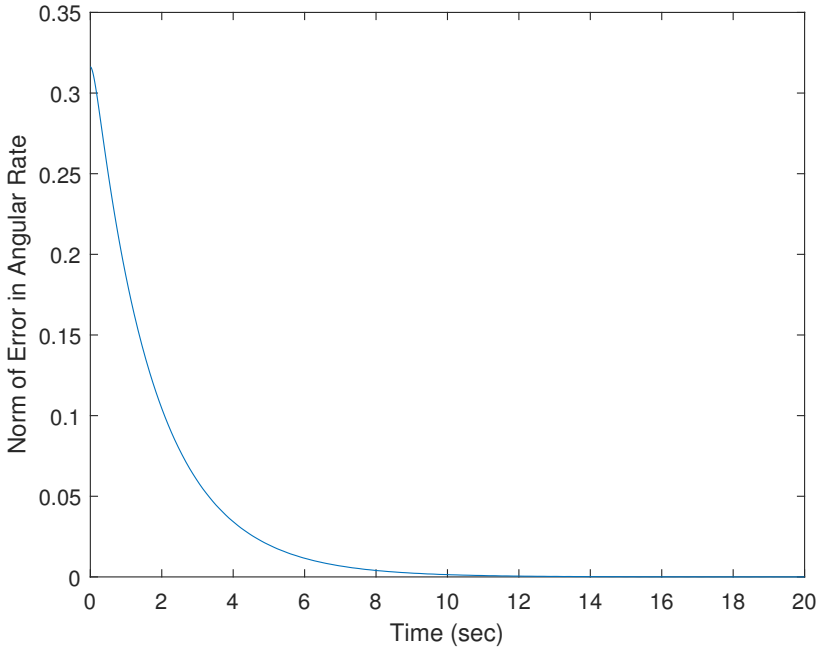

(a) Norm of difference in true and estimated angular velocities

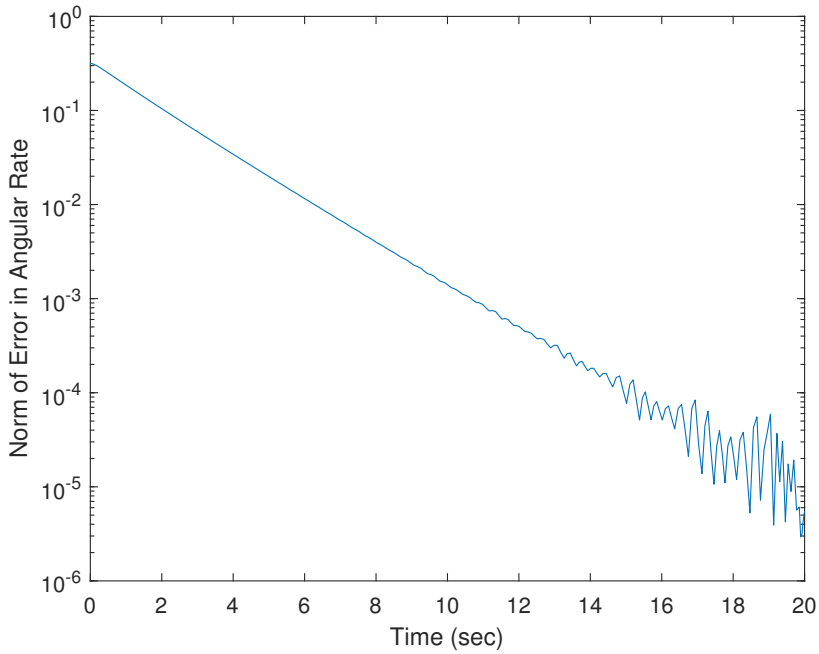

(b) Norm of the angular velocity estimation error

Figure 1: Simulations for the known torque and inertia case

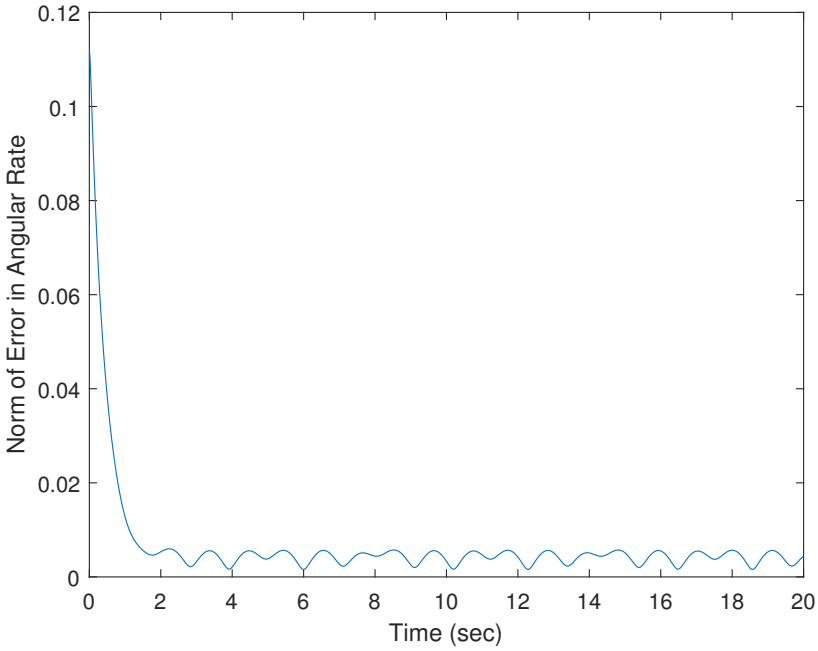

(a) Norm of difference in true and estimated angular velocities

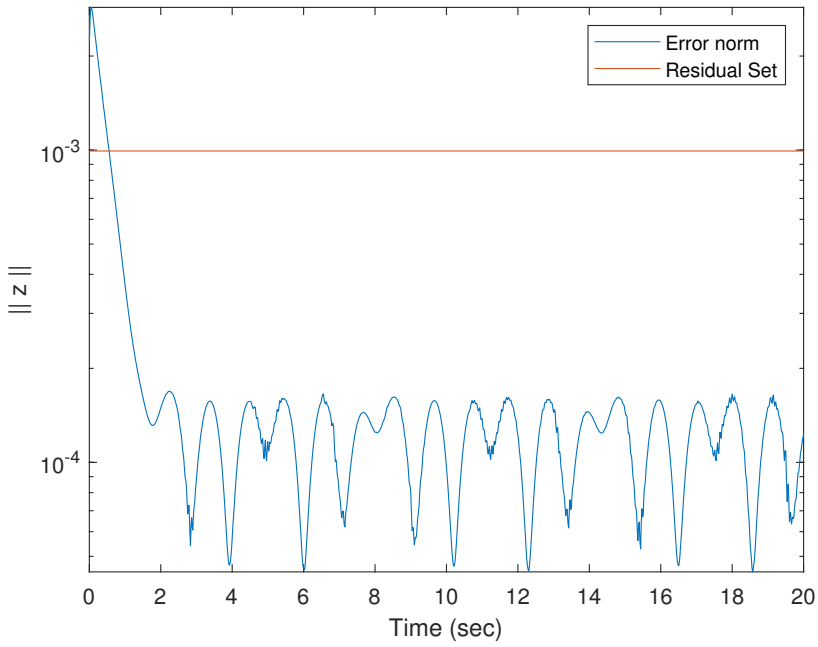

(b) Norm of Error states

Figure 2: Simulations for the inaccurate inertia and unknown torque case

CONCLUSIONS

A novel observer was designed for estimating the full attitude and angular rate states from the continuous measurements of a Rate Integrating Gyroscope (RIG). The observer was shown using a Lyapunov-like analysis to drive the angular velocity estimates to their true values exponentially fast. The update laws are linear in the measurement term and involve one user chosen parameter which controls the convergence rate of the estimate and the region of attraction for the initial value of the state. The observer was also shown to be robust to an inaccurately modeled inertia matrix as well as unknown torque inputs to the system. The effectiveness of the design was proven numerically in simulations. Future work will focus on estimating the inertia matrix as well for the unknown inertia case.

REFERENCES

[1] P. G. Savage, "Strapdown inertial navigation integration algorithm design part 2: Velocity and position algorithms," *Journal of Guidance, Control, and Dynamics*, Vol. 21, No. 2, 1998, pp. 208–221.

[2] J. L. Crassidis, F. L. Markley, and Y. Cheng, "Survey of Nonlinear Attitude Estimation Methods," *Journal of Guidance, Control, and Dynamics*, Vol. 30, No. 1, 2007, pp. 12–28, 10.2514/1.22452.

[3] J. C. Kinsey, R. M. Eustice, and L. L. Whitcomb, "A survey of underwater vehicle navigation: Recent advances and new challenges," *IFAC Conference of Manoeuvering and Control of Marine Craft*, Vol. 88, Lisbon, 2006, pp. 1–12.

[4] N. Fallah, I. Apostolopoulos, K. Bekris, and E. Folmer, "Indoor human navigation systems: A survey," *Interacting with Computers*, Vol. 25, No. 1, 2013, pp. 21–33.

[5] B. Barshan and H. F. Durrant-Whyte, "Inertial navigation systems for mobile robots," *IEEE transactions on robotics and automation*, Vol. 11, No. 3, 1995, pp. 328–342.

[6] F. L. Markley and J. L. Crassidis, *Fundamentals of spacecraft attitude determination and control*, Vol. 33. Springer, 2014.

[7] D. Senkal, E. Ng, V. Hong, Y. Yang, C. Ahn, T. Kenny, and A. Shkel, "Parametric drive of a toroidal MEMS rate integrating gyroscope demonstrating¡ 20 PPM scale factor stability," *2015 28th IEEE International Conference on Micro Electro Mechanical Systems (MEMS)*, IEEE, 2015, pp. 29–32.

[8] P. Pai, H. Pourzand, and M. Tabib-Azar, "Magnetically coupled resonators for rate integrating gyroscopes," *SENSORS, 2014 IEEE*, IEEE, 2014, pp. 1173–1176.

[9] J. L. Crassidis and F. L. Markley, "Three-axis attitude estimation using rate-integrating gyroscopes," *Journal of Guidance, Control, and Dynamics*, Vol. 39, No. 7, 2016, pp. 1513–1526.

[10] B. Friedkand, "Estimating Angular Velocity from Output of Rate-integrating Gyro," *IEEE Transactions on Aerospace and Electronic Systems*, Vol. AES-11, No. 4, 1975, pp. 551–555, 10.1109/TAES.1975.308119.

[11] H. F. Grip, T. I. Fossen, T. A. Johansen, and A. Saberi, "Globally exponentially stable attitude and gyro bias estimation with application to GNSS/INS integration," *Automatica*, Vol. 51, 2015, pp. 158 – 166.

[12] S. Berkane, A. Abdessameud, and A. Tayebi, "A globally exponentially stable hybrid attitude and gyro-bias observer," *2016 IEEE 55th Conference on Decision and Control (CDC)*, 2016, pp. 308–313.

[13] H. K. Khalil and J. W. Grizzle, *Nonlinear systems*, Vol. 3. Prentice hall Upper Saddle River, NJ, 2002.